

Reaction Rate Constants from Classical Trajectories of Atom-Diatomic Molecule Collisions

Hamzeh M. Abdel-Halim and Sawsan M. Jaafreh

The Hashemite University, Faculty of Science, Department of Chemistry, P.O. Box 330127, Zarqa 13133, Jordan

Reprint requests to Dr. H. M. A.-H.; E-mail: hamzehah@hu.edu.jo

Z. Naturforsch. **63a**, 159–169 (2008); received August 27, 2007

Classical trajectory calculations for various atom-diatomic molecules were performed using the three-dimensional Monte Carlo method. The reaction probabilities, cross-sections and rate constants of several systems were calculated. Equations of motion, which predict the positions and momenta of the colliding particles after each step, have been integrated numerically by the Runge-Kutta-Gill and Adams-Moulton methods. Morse potential energy surfaces were used to describe the interaction between the atom and each atom in the diatomic molecules. The results were compared with experimental ones and with other theoretical values. Good agreement was obtained between calculated rate constants and those obtained experimentally. Also, reasonable agreement was observed with theoretical rate constants obtained by other investigators using different calculation methods. The effects of the temperature, the nature of the colliding particles and the thermochemistry were studied. The results showed a strong dependence of the reaction rates on these factors.

Key words: Rates; Atom-Diatomic Molecule; Collisions; Classical Trajectories.

1. Introduction

Collisions between molecules or between atoms and molecules are important events from the physical and chemical points of view. They may be elastic or inelastic. Inelastic collisions involve the field of reactive collisions which is of particular importance and interest: chemical reactions between atoms and molecules can be studied using theoretical methods. For reactive collisions between an atom (A) and a diatomic molecule (BC), the process is simplified by bond breaking of BC and bond formation of AB or AC. Such collisions can be studied using quantum, classical or semi-classical mechanical methods. The quantum mechanical solution is done by solving the Schrödinger equation; $\hat{H}\Psi = E\Psi$, where \hat{H} is the Hamiltonian operator, Ψ the wave function and E the energy. Solving this equation is difficult because an exact wave function for the system is hard to find. On the other hand, classical methods of calculation are easier to carry out, and they are well established. The classical solution involves classical trajectories by solving Hamilton's equations of motion in order to determine the position and the momentum of each of the colliding particles in every step of the trajectory during the collision. In the present work, a semi-classical method was employed, in which

classical trajectories evolving on potential surfaces, whose parameters are determined quantum mechanically, were used.

The classical trajectories method has been widely used to study reactive collisions between atoms and diatomic molecules [1–17]. It provides a reliable method for the calculation of the reaction probability, from which the reaction cross-section and rate constant can be calculated. This method is frequently used to compare theoretical with experimental results. Several calculations in this category have been reported; Zuhrt et al. [1] used quasi-classical trajectory (QCT) calculations for the reaction of $\text{He} + \text{H}_2^+$. They studied the effect of the reactants' translational, vibrational, and rotational energies on reaction cross-sections. Their results showed that higher vibrational energy of the diatomic molecule is more effective in promoting the reaction than translational energy. Using their *ab initio* potential energy surface, Lester and Schinke [2] reported rate constant calculations for the reaction of $\text{O}(^3\text{P})$ with H_2 . Their calculations were in good agreement with the experimental rate constant at 302 K. Using classical trajectory calculations, Luntz et al. [3] reported a study of the upper atmosphere reaction: $\text{O}(^1\text{D}) + \text{H}_2$. The objective of their study was to predict the dynamics of the reaction and to compare the

results with values obtained using scattering calculations. The ion-molecule reaction: $O^- + D_2$, was studied at relatively high energies by Herbst et al. [4]. Jaffe [5] reported theoretical rate constants for the atmospherically important reaction: $ClO + O$, using classical trajectory calculations. The calculated rate constant and activation energy were found to be in good agreement with the experimental values. Persky [6] reported the rate constants, isotope effects, and energy disposal features for the $Cl + HD$ reaction. Semi-classical calculations of the thermal rate constants in full Cartesian space for the reaction: $D + H_2 \rightarrow DH + H$, were performed by Yamamoto and Miller [7]. A paper on the comparative role of the potential energy surface in classical, semi-classical and quantum mechanical calculations for atom-diatomic reactive collisions has been published by Judson et al. [8]. Thompson et al. [9] did cross-section calculations for the complex formation in $H + OH$ collisions. Hutchinson and Wyatt [10] studied the collinear collision for the reaction $F + H_2$, to investigate the classical versus quantum and classical versus statistical behaviour of the reaction. A three-dimensional (3-D) quasi-classical trajectory study to evaluate the rate constants of the reactions: $H + ClF$, $F + HCl$, $D + ClF$, $F + DCl$, was presented by Sayos et al. [11]. Using a quasi-classical trajectory, Truhlar [12] discussed the reliability of several practical techniques for computing the equilibrium rate constant of the reactions: $H + H_2$, $Cl + H_2$, $H + Cl_2$, $F + H_2$, $I + H_2$, and their isotopic analogues within 300–1500 K. Paul et al. [13] studied the isotope dependence of the $O + O_2$ exchange reaction by means of kinetic experiments and by classical trajectory calculations. Their measurements confirmed a previously reported negative temperature dependence. They reported rate coefficients for the exothermic $^{18}O + ^{16}O_2 \rightarrow ^{18}O^{16}O + ^{16}O$ and the endothermic $^{16}O + ^{18}O_2 \rightarrow ^{16}O^{18}O + ^{18}O$ reaction between 233 and 253 K. Gray and Truhlar [14] studied the thermal collinear reaction rates for $H + Cl_2 \rightarrow HCl + Cl$ using trajectory calculations. Connor et al. [15] compared a quasi-classical transition state theory and quantum mechanical calculations of the rate constants and the activation energies for the collinear reaction: $X + F_2 \rightarrow XF + F$, where $X = Mu, H, D, T$. Direct Monte Carlo quasi-classical trajectory calculations were performed by Muckerman and Faist [16] to calculate the rate constants for three chemical reactions: $F + H_2$, $Cl + H_2$, and $O(^3P) + H_2$, at several temperatures. Porter et al. [17] used a quasi-classical procedure for the examination of the colli-

sion dynamics of $H + H_2$ reactions by means of Monte Carlo averages over a large number of classical trajectories. The total reaction cross-section was determined as a function of initial relative velocity and the initial molecular vibrational-rotational state.

In the present work, the reaction probability, of several systems was studied for atom-diatomic molecule collisions using the Monte Carlo semi-classical trajectory method. Morse potential energy surfaces were applied for the interactions between the atom and the diatomic molecule. The probability of the reaction, the reaction cross-section and the rate constant were calculated for various initial values of the dynamical variables. The calculated values were compared with experimental values. All calculations were performed using a FORTRAN compiler from Salford University.

2. Method of Calculation

The use of the classical trajectory method to calculate reaction probabilities involves solving numerically Hamilton's equations of motion for the colliding particles. Hamilton's equations for the generalized coordinates Q_j and momenta P_j are given by

$$\begin{aligned} \frac{dQ_j}{dt} &= \dot{Q}_j = \frac{\partial H'}{\partial P_j} = \frac{\partial T}{\partial P_j}, \\ \frac{dP_j}{dt} &= \dot{P}_j = -\frac{\partial H'}{\partial Q_j} = -\frac{\partial V}{\partial Q_j}, \end{aligned} \quad (1)$$

where H' is the classical Hamiltonian that equals to the sum of the kinetic energy operator, T , and the potential energy operator, V . The numerical integration solution of Hamilton's equations determines the position, Q_j , and the momentum, P_j , for each particle as a function of time during the pathway of the trajectory. For a three-body system with the atom A and the atoms B and C of the molecule BC, the point masses m_A , m_B and m_C , the Cartesian coordinates (q_1, q_2, q_3) , (q_4, q_5, q_6) and (q_7, q_8, q_9) , and the conjugate momenta (p_1, p_2, p_3) , (p_4, p_5, p_6) and (p_7, p_8, p_9) , respectively, the Hamiltonian function of a potential $V(q_1, q_2, \dots, q_9)$ has the form

$$\begin{aligned} H' &= \frac{1}{2m_A} \sum_{i=1}^3 p_i^2 + \frac{1}{2m_B} \sum_{i=4}^6 p_i^2 \\ &+ \frac{1}{2m_C} \sum_{i=7}^9 p_i^2 + V(q_1, q_2, \dots, q_9). \end{aligned} \quad (2)$$

Simplification of the problem can be done by using relative coordinates and momenta (Q' 's and P' 's) instead of

absolute coordinates and momenta (q 's and p 's). This reduces the number of parameters to be solved from 18 to 12. Relative coordinates are related to absolute coordinates by the relations

$$\begin{aligned} Q_j &= q_{j+6} - q_{j+3}, \\ Q_{j+3} &= q_j - (m_B q_{j+3} + m_C q_{j+6}) / (m_B + m_C), \\ Q_{j+6} &= (1/M) (m_A q_j + m_B q_{j+3} + m_C q_{j+6}) \\ (j &= 1, 2, 3), \end{aligned} \quad (3)$$

where $M = m_A + m_B + m_C$. Also, the relations between the relative and absolute momenta are given by

$$\begin{aligned} p_i &= P_{i+3} + (m_A/M) P_{i+6}, \\ p_{i+3} &= -P_i - [m_B / (m_B + m_C)] P_{i+3} \\ &\quad + (m_B/M) P_{i+6}, \\ p_{i+6} &= P_i - [m_C / (m_B + m_C)] P_{i+3} \\ &\quad + (m_C/M) P_{i+6} \quad (i = 1, 2, 3). \end{aligned} \quad (4)$$

Here, the coordinate system is the same as the one employed by Porter et al. [17]. Using relative coordinates and momenta, (2) becomes

$$\begin{aligned} H' &= \frac{1}{2\mu_{BC}} \sum_{j=1}^3 P_j^2 + \frac{1}{2\mu_{A,BC}} \sum_{j=4}^6 P_j^2 \\ &\quad + V(Q_1, \dots, Q_6), \end{aligned} \quad (5)$$

where μ_{BC} is the reduced mass of the atoms B and C and $\mu_{A,BC}$ is the reduced mass of the atom A and the molecule BC. In (5), (Q_1, Q_2, Q_3) , (P_1, P_2, P_3) represent the Cartesian coordinates and conjugate momenta, respectively, of atom B with respect to atom C as origin, and (Q_4, Q_5, Q_6) , (P_4, P_5, P_6) are the Cartesian coordinates and conjugate momenta of atom A with respect to the centre of mass of the pair (B, C) as origin. The interatomic separations: A–B (R_1), B–C (R_2), and A–C (R_3), are related to coordinates Q_j ($j = 1, 2, \dots, 6$) by the relations

$$\begin{aligned} R_1 &= [(q_4 - q_1)^2 + (q_5 - q_2)^2 + (q_6 - q_3)^2]^{1/2} \\ &= \left[\left(\frac{m_C}{m_B + m_C} Q_1 + Q_4 \right)^2 + \left(\frac{m_C}{m_B + m_C} Q_2 + Q_5 \right)^2 \right. \\ &\quad \left. + \left(\frac{m_C}{m_B + m_C} Q_3 + Q_6 \right)^2 \right]^{1/2}, \\ R_2 &= [(q_7 - q_4)^2 + (q_8 - q_5)^2 + (q_9 - q_6)^2]^{1/2} \\ &= (Q_1^2 + Q_2^2 + Q_3^2)^{1/2}, \end{aligned}$$

$$\begin{aligned} R_3 &= [(q_7 - q_1)^2 + (q_8 - q_2)^2 + (q_9 - q_3)^2]^{1/2} \\ &= \left[\left(\frac{m_B}{m_B + m_C} Q_1 - Q_4 \right)^2 + \left(\frac{m_B}{m_B + m_C} Q_2 - Q_5 \right)^2 \right. \\ &\quad \left. + \left(\frac{m_B}{m_B + m_C} Q_3 - Q_6 \right)^2 \right]^{1/2}. \end{aligned} \quad (6)$$

Using the chain rule

$$\frac{\partial V}{\partial Q_j} = \sum_k \frac{\partial V}{\partial R_k} \frac{\partial R_k}{\partial Q_j}, \quad (7)$$

Hamilton's equations of motion will have the form

$$\begin{aligned} \dot{Q}_j &= (1/\mu_{BC}) P_j \quad (j = 1, 2, 3), \\ \dot{Q}_j &= (1/\mu_{A,BC}) P_j \quad (j = 4, 5, 6), \end{aligned} \quad (8)$$

$$\begin{aligned} -\dot{P}_j &= \frac{1}{R_1} \frac{m_C}{m_B + m_C} \left(\frac{m_C}{m_B + m_C} Q_j + Q_{j+3} \right) \frac{\partial V}{\partial R_1} \\ &\quad + \frac{Q_j}{R_2} \frac{\partial V}{\partial R_2} + \frac{1}{R_3} \frac{m_B}{m_B + m_C} \left(\frac{m_B}{m_B + m_C} Q_j - Q_{j+3} \right) \frac{\partial V}{\partial R_3} \\ &\quad (j = 1, 2, 3), \\ -\dot{P}_j &= \frac{1}{R_1} \left(\frac{m_C}{m_B + m_C} Q_j + Q_{j+3} \right) \frac{\partial V}{\partial R_1} \\ &\quad - \frac{1}{R_3} \left(\frac{m_B}{m_B + m_C} Q_j - Q_{j+3} \right) \frac{\partial V}{\partial R_3} \\ &\quad (j = 4, 5, 6). \end{aligned} \quad (9)$$

From the above equation, the net Hamiltonian equations will be

$$\begin{aligned} H' &= \frac{1}{2\mu_{BC}} \sum_{j=1}^3 P_j^2 + \frac{1}{2\mu_{A,BC}} \sum_{j=4}^6 P_j^2 \\ &\quad + V(R_1, R_2, R_3) \end{aligned} \quad (10)$$

with 12 simultaneous differential equations to be integrated for the determination of the time variation of Q_j and P_j .

2.1. Initial Values of the Dynamical Variables

The twelve dynamical variables [Q_j and P_j ($j = 1, 2, \dots, 6$)] have to be specified to define the initial state of a collision trajectory. If the z -axis is chosen as the direction of the initial relative velocity of atom A towards the BC molecule (\mathbf{v}_{rel}), i. e. $\mathbf{v}_{\text{rel}} = \mathbf{v}_z$ and $\mathbf{v}_x = \mathbf{v}_y = 0$, then

$$\begin{aligned} P_x &= P_4^0 = \mu_{A,BC} v_x = 0, \\ P_y &= P_5^0 = \mu_{A,BC} v_y = 0, \\ P_z &= P_6^0 = \mu_{A,BC} v_z = \mu_{A,BC} v_{\text{rel}}, \end{aligned} \quad (11)$$

with v_{rel} equals to $(2E_{\text{trans}}/\mu_{\text{A,BC}})^{1/2}$, where E_{trans} is the translation energy. If the orientation of atom A and the centre of mass of BC is chosen to be in the yz -plane, then

$$Q_4^0 = 0, \quad Q_5^0 = b, \quad Q_6^0 = -(R_{\text{max}}^2 - b^2)^{1/2}, \quad (12)$$

where b is the impact parameter, which is the distance of the closest approach of A from BC, and R_{max} is the initial distance between atom A and the centre of the mass of BC. At this distance the interaction of A with BC is negligible.

The orientation of BC is specified by the polar coordinates, such that

$$\begin{aligned} Q_1^0 &= r \sin \theta \cos \phi, \\ Q_2^0 &= r \sin \theta \sin \phi, \\ Q_3^0 &= r \cos \theta, \end{aligned} \quad (13)$$

where r is the initial internuclear separation of the molecule BC, and θ and ϕ are the angles that define the orientation of BC in the three-atom polar coordinate system. In the present work, the two classical turning points of the diatomic molecule (r_{\pm}) were chosen alternatively to be the initial values of r . From the classical point of view, at the turning points the molecular speed is zero. Hence, the probability of finding the molecule at these points is maximal. This restriction in the initial molecular internuclear distance considerably simplifies the selection of the internal momentum components for the molecule and produces *no* loss of generality because of the alternative choice of the minimum and maximum separations. For our own curiosity reason, a micro-canonical simulation was tested. Using the same calculation method, a large number of points between minimum and maximum separations were tried. The results were averaged over the total number of reactive trajectories. The method is tedious and does *not* produce a significant improvement with experimental values. To determine the values of r_+ and r_- , the vibrational potential energy for the diatomic molecule is represented by a Morse function, and the values of (r_{\pm}) that satisfy the following equation were found:

$$\begin{aligned} D_2[1 - \exp\{-\alpha_2(R_2 - Re_2)\}]^2 \\ + J(J+1)\hbar^2/2\mu_{\text{BC}} = E_{v,J}, \end{aligned} \quad (14)$$

where $E_{v,J}$ is the initial internal energy of the molecule defined by the vibrational quantum number v and

the rotational quantum numbers J . The constants D_2 , α_2 , and Re_2 are the spectroscopic constants of the BC molecule.

The total internal molecular momentum P has two components:

$$P^2 = P_{\theta}^2 + P_r^2, \quad (15)$$

where P_{θ}^2 is the angular momentum that is perpendicular to the bond BC, which is due to the rotational motion, and P_r^2 is the parallel momentum along the bond direction and is due to the vibrational motion. The total momentum is related to its initial components by the relation

$$P^2 = (P_1^0)^2 + (P_2^0)^2 + (P_3^0)^2. \quad (16)$$

To completely specify the internal momentum components, P_j^0 ($j = 1, 2, 3$), an angle β is needed to be fixed; β is the angle of the momentum vector relative to an arbitrarily chosen vector that is perpendicular to the molecular axis. If this vector is taken to be $\mathbf{R} \times \mathbf{\kappa}$, where \mathbf{R} points along the molecular axis and $\mathbf{\kappa}$ is the unit vector in the z -direction, then

$$\begin{aligned} P_1^0 &= P_r \sin \theta \cos \phi - P_{\theta}(\sin \phi \cos \beta + \cos \phi \cos \theta \sin \beta), \\ P_2^0 &= P_r \sin \theta \cos \phi + P_{\theta}(\cos \phi \cos \beta - \sin \phi \cos \theta \sin \beta), \\ P_3^0 &= P_r \cos \phi + P_{\theta} \sin \theta \sin \beta. \end{aligned} \quad (17)$$

At turning points there is no momentum component along the bond direction. At this point the velocity is zero and $P_r = \mu_{\text{A,BC}} v_{\text{rel}} = 0$. The total internal molecular momentum is simply related to the angular momentum, such that

$$P^2 = J(J+1)\hbar^2/r_{\pm}^2. \quad (18)$$

Equation (17) becomes

$$\begin{aligned} P_1^0 &= -P_{\theta}(\sin \phi \cos \beta + \cos \phi \cos \theta \sin \beta), \\ P_2^0 &= P_{\theta}(\cos \phi \cos \beta - \sin \phi \cos \theta \sin \beta), \\ P_3^0 &= P_{\theta} \sin \theta \sin \beta. \end{aligned} \quad (19)$$

Thus, the initial state of a trajectory is defined by specifying values for the dynamical variables: r_{\pm} , θ , ϕ , β , b , R_{max} , J , v , v_{rel} , and the spectroscopic constants for AB, BC, and AC. In the present work, the values of θ , ϕ , β , and b were selected randomly by Monte Carlo techniques [18], while values of the other parameters

were assigned arbitrarily. The values of b , θ , ϕ , and β are given by

$$\begin{aligned} b &= b_{\max} \xi^{1/2}, & \theta &= 2\xi - 1, \\ \phi &= 2\pi\xi, & \beta &= 2\pi\xi, \end{aligned} \quad (20)$$

where b_{\max} is the maximum impact parameter beyond which no significant interaction between A and BC occurs, and ξ is a random number, obtained by using random number generator software, having values between 0 and 1. The initial rotational and vibrational energies of the diatomic molecule were calculated from the assigned J and ν values, such that

$$\begin{aligned} E_{\text{rot}} &= P_{\theta}^2 / 2\mu_{\text{BC}} = (\hbar^2 / 2\mu_{\text{BC}} r_{\pm}^2) J(J+1), \\ E_{\text{vib}} &= D_2 [1 - \{1 - \alpha_2 (\hbar^2 / 2\mu_{\text{BC}} D_2)^{1/2}\} \\ &\quad \cdot (\nu + 1/2)]. \end{aligned} \quad (21)$$

Here, the term for E_{vib} was obtained from the solution of the Schrödinger equation using the WKB approximation [19].

2.2. Potential Energy Surfaces

In the present work, Morse potential energy surfaces are used to describe the interaction between atoms involved in the collision process, given by

$$\begin{aligned} V_{\text{AB}} &= D_1 [1 - \exp\{-\alpha_1 (R_1 - Re_1)\}]^2 - D_1, \\ V_{\text{BC}} &= D_2 [1 - \exp\{-\alpha_2 (R_2 - Re_2)\}]^2 - D_2, \\ V_{\text{AC}} &= D_3 [1 - \exp\{-\alpha_3 (R_3 - Re_3)\}]^2 - D_3, \end{aligned} \quad (22)$$

where V_{AB} , V_{BC} and V_{AC} are the potentials between atom pairs (A–B), (B–C) and (A–C), respectively. The constants D_j , α_j and Re_j ($j = 1, 3$) are the spectroscopic constants for AB and AC molecules, respectively.

After specifying the initial values of the dynamical variables and choosing the potential energy surfaces between interacting atoms, the classical trajectory can be started. Hamilton's equations of motions were integrated numerically by the Runge-Kutta-Gill [20] (RKG) fourth-order method and the Adams-Moulton [20] (AM) corrector and predictor method. To reduce computer time, the first five cycles of each trajectory were done by the RKG method, then, the integration was shifted to a higher gear using the AM method. The integration interval size used was chosen between $2.15 \cdot 10^{-15}$ and $2.15 \cdot 10^{-16}$ s. The accuracy

of the numerical integration was checked by the following methods: First, by the constancy of the total energy throughout the trajectory, which serves as a crude test for the integration accuracy for a non-reactive collision. Second, by the back-integration method, in which the direction of the momenta at the end of the trajectory is reversed and then integrated back to the initial state. Third, by comparing results of several trajectories that have the same initial states but different integration interval sizes.

2.3. Final State Analysis

As the trajectory proceeds, atom A starts moving in steps towards the BC molecule. After each step, new Q_j 's and P_j 's ($j = 1, 2, \dots, 6$) are determined by the numerical integration. The distance of A from the centre of mass of BC keeps decreasing until it reaches a minimum, at which the interaction of A with both B and C is maximal. At this point the probability of a reaction to occur is maximal. Depending on whether a reaction occurs or not, an atom (A, B, C) starts moving away from the molecule (BC, AC, AB) until it reaches a distance where its interaction with both atoms of the molecule is negligible. The trajectory ends when either R_1 , R_2 or R_3 equals to or is greater than R_{\max} . At the end of the trajectory, the potential values between atomic pairs V_{AB} , V_{BC} and V_{AC} determine whether a reaction occurs or not. If V_{BC} is greater than both V_{AB} and V_{AC} , no reaction occurs. In this case atom A collides and then flies away from the BC molecule. Here, exchange of energy between A and BC may or may not occur, depending on whether the collision is inelastic or elastic, respectively. On the other hand, if V_{AB} is greater than both V_{BC} and V_{AC} , then a reaction occurs and an AB molecule is produced. However, if V_{AC} is greatest, the molecule AC forms.

The final status of the system can be defined using the final values of Q_j and P_j ($j = 1, 2, \dots, 6$). For a non-reactive collision, the final relative velocity of the free atom A is determined from the final P_j 's ($j = 1, 2, 3$), and it is given by

$$v'_j = [(m_A + m_B + m_C) / m_A (m_B + m_C)] P_{j+3}, \quad (23)$$

where $j = 1, 2, 3$ correspond to the x -, y -, z -components, respectively. The final relative energy is determined from the final relative velocity, given by

$$E'_{\text{rel}} = 0.5 \mu_{\text{A,BC}} (v_x'^2 + v_y'^2 + v_z'^2). \quad (24)$$

The final angular momentum of the molecule BC is determined from the final Q_j 's and P_j 's ($j = 1, 2, 3$), such that

$$\begin{aligned} L'_x &= Q_2P_3 - Q_3P_2, \\ L'_y &= Q_3P_1 - Q_1P_3, \\ L'_z &= Q_1P_2 - Q_2P_1. \end{aligned} \quad (25)$$

From the final angular momentum of BC, the final rotational energy of the molecule is determined; it is given by

$$E'_{\text{rot}} = (L'^2_x + L'^2_y + L'^2_z)/2\mu_{\text{BC}}R_{\text{BC}}^2. \quad (26)$$

The final internal energy, which is the sum of the rotational and vibrational energy [19], is given by

$$E'_{\text{int}} = [(P_1^2 + P_2^2 + P_3^2)/2\mu_{\text{BC}}] + V_{\text{M}}(R_{\text{BC}}). \quad (27)$$

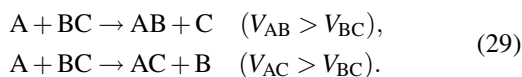
And the final vibrational energy of the molecule is given by

$$E'_{\text{vib}} = E'_{\text{int}} - E'_{\text{rot}}. \quad (28)$$

A similar treatment is applied for a reactive collision. The free atom is B or C when the produced molecule is AC or AB, respectively.

2.4. Reaction Probability, Cross-Section and Rate Constant

In the trajectory, when the distance between atom A and the centre of mass of the molecule BC is at a minimum, the interaction of A with both B and C has a maximum value. At this point it is possible that the interaction potential between A and B or between A and C becomes greater than that between B and C. In this case, the bond B-C will break and a bond will form between A and B or A and C according to



The corresponding probabilities at a given temperature T , $P(T)$, are given by

$$\begin{aligned} P_{\text{AB}}(T) &= \frac{\text{number of AB produced}}{\text{total number of trajectories}}, \\ P_{\text{AC}}(T) &= \frac{\text{number of AC produced}}{\text{total number of trajectories}}. \end{aligned} \quad (30)$$

The rate of the reaction in (29) is given by

$$R = k(T)[\text{A}][\text{BC}], \quad (31)$$

where $k(T)$ is the rate constant. The reaction rate can be calculated from the collision theory [21, 22], given by

$$R = R_{\text{C}}e^{-E_0/k_{\text{B}}T}, \quad (32)$$

where E_0 is the barrier energy, which is the threshold energy for the reaction to occur. For an exothermic reaction, which is the case for most reactions studied in the present work, $E_0 = 0$. For endothermic reactions, literature values of E_0 were used. The collision rate of the reaction, R_{C} , is given by

$$R_{\text{C}} = \bar{v}_{\text{rel}}\sigma[\text{A}][\text{BC}], \quad (33)$$

where \bar{v}_{rel} is the average relative velocity, given by

$$\bar{v}_{\text{rel}} = \left(\frac{8k_{\text{B}}T}{\pi\mu_{\text{A,BC}}} \right)^{1/2}, \quad (34)$$

where σ is the collision cross-section, given by

$$\sigma = \pi d^2. \quad (35)$$

Here d is the collision diameter, such that

$$d = 0.5(d_{\text{A}} + d_{\text{BC}}), \quad (36)$$

where d_{A} and d_{BC} are the collision diameter of atom A and molecule BC.

Using (31)–(36), the rate constant is given by

$$k(T) = \bar{v}_{\text{rel}}\sigma e^{-E_0/k_{\text{B}}T}. \quad (37)$$

The collision theory treats molecules as *structureless* spheres. The major problem with this model is that the observed pre-exponential factor in (37) is some times much smaller than the gas kinetic collision rate. Introducing the reaction cross-section σ_{r} solves the problem. The reaction cross-section is related to the collision cross-section by the relation

$$\sigma_{\text{r}} = P(T)\sigma, \quad (38)$$

where $P(T)$ is the reaction probability, which has a value between 0.0 and 1.0 and is given by

$$P(T) = \frac{\text{number of trajectories that lead to reaction}}{\text{total number of trajectories}}. \quad (39)$$

Equation (37) becomes

$$k(T) = \bar{v}_{\text{rel}}\sigma_{\text{r}}e^{-E_0/k_{\text{B}}T}. \quad (40)$$

Equations (38)–(40) were used to calculate the reaction cross-section, probability and rate constants for systems studied in the present work.

3. Results and Discussion

For each reactive collision studied a large number of trajectories were performed to mimic the experimental situation. Depending on the reaction temperature, the step size of integration selected, and other initial parameters, the number of trajectories performed was between 10,000–60,000. The maximum number of trajectories is chosen when there is no significant change in the results produced (less than 2%). Only “good trajectories” were included in the calculations. A “good trajectory” is one that passes the accuracy check (mentioned earlier) and has less than 1.0% errors. Each trajectory is unique by the set of its initial values of the dynamical variables, which were chosen randomly. The spectroscopic constants for each atomic pair were chosen carefully from literature [23–25]. Various values were reported. Only trusted and repeated values were selected. Effects of all spectroscopic constants of the molecule have been studied in a previous work [19]. Regarding the well depth, we did the calculations by varying its value by up to 10%. We observed *no* significant change in the results. Considering this, and considering other sources of errors mentioned earlier, we believe that our reported rate constants have less than 3% errors. Unless otherwise stated, the reactions were studied at 300 K. The initial vibrational and rotational quantum numbers selected for molecules were: $v = 0$ and J_{\max} , where J_{\max} is the rotational level of maximum population for the molecule at a given temperature. The calculated reaction probabilities and cross-sections for the systems studied in the present work are shown in Table 1. Results of the calculations of rate constants, along with experimental and other theoretical values obtained at the same conditions, are shown in Table 2. Below are details for each reactive collision studied.

3.1. Reactions of Hydrogen Atoms with Different Diatomic Molecules

Rate constants of various reactions involving hydrogen or deuterium atoms were calculated. The results were compared with experimental values and/or with other theoretical results calculated using different methods. The reactions studied in this category were:

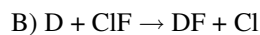


This reaction was studied at 300 K. The barrier energy of this exothermic reaction is $E_0 = 0$. A step

Table 1. Calculated probabilities and reaction cross-sections for various collision partners at 300 K.

System	$P(T)$	$\sigma_r [\text{\AA}^2]$
$\text{H} + \text{ClF} \rightarrow \text{HF} + \text{Cl}$	0.0364	0.456
$\text{D} + \text{ClF} \rightarrow \text{DF} + \text{Cl}$	0.0131	0.164
$\text{H} + \text{ClF} \rightarrow \text{HCl} + \text{F}$	0.0954	1.20
$\text{D} + \text{ClF} \rightarrow \text{DCl} + \text{F}$	0.103	1.30
$\text{H} + \text{ICl} \rightarrow \text{HCl} + \text{I}$	0.0833	1.89
$\text{H} + \text{F}_2 \rightarrow \text{HF} + \text{F}$	0.0142	0.141
$\text{H} + \text{Cl}_2 \rightarrow \text{HCl} + \text{Cl}$	0.0559	0.977
$\text{F} + \text{HCl} \rightarrow \text{HF} + \text{Cl}$	0.0999	1.24
$\text{F} + \text{DCl} \rightarrow \text{DF} + \text{Cl}$	0.0891	1.10
$\text{F} + \text{HBr} \rightarrow \text{HF} + \text{Br}$	0.485	6.88
$\text{F} + \text{HI} \rightarrow \text{HF} + \text{I}$	0.394	6.63
$\text{F} + \text{H}_2 \rightarrow \text{HF} + \text{H}$	0.0571	0.378
$\text{Cl} + \text{HD} \rightarrow \text{HCl} + \text{D}$	0.0711	0.670
$\text{Cl} + \text{DH} \rightarrow \text{DCl} + \text{H}$	0.182	1.71
$\text{Cl} + \text{H}_2 \rightarrow \text{HCl} + \text{H}$	0.0797	0.751

size of $4.1 \cdot 10^{-16}$ s throughout the trajectory was chosen. An initial distance of 10.0 Å of H from the centre of mass of ClF with a maximum impact parameter (b_{\max}) of 5.0 Å was selected. At these conditions, with more than 60,000 trajectories computed, the calculations yielded a probability of 0.0364 for this reaction to occur with a reaction cross-section of 0.456 \AA^2 . The obtained rate constant for this reaction was $11.6 \cdot 10^{-12} \text{ cm}^3 \text{ molecule}^{-1} \text{ s}^{-1}$. This value is in excellent agreement with the experimental value of $(12.0 \pm 1.0) \cdot 10^{-12} \text{ cm}^3 \text{ molecule}^{-1} \text{ s}^{-1}$ reported by Bykhalo and coworkers [26]. However, the agreement is not as good with other experimental values [27, 28]. Discrepancies between experimental values are due to different experimental techniques employed. This reaction was also studied theoretically by other investigators [11] using 3D quasi-classical trajectory studies on a new (${}^2A'$) *ab initio* potential energy surface. Poor agreement was observed between their calculated rate constant $[(6.7 \pm 0.10) \cdot 10^{-12} \text{ cm}^3 \text{ molecule}^{-1} \text{ s}^{-1}]$ and the one obtained in this work. It is unwise to indicate which calculation method is more accurate. Taking into consideration the complexity of the calculations in both procedures makes the difference between the two results acceptable.



This reaction was studied to see the isotope effect on a reaction rate. Similar initial conditions as in the previous reaction were selected. The reaction probability and cross-section are listed in Table 1. As expected, the rate constant of the heavier isotope D, is smaller than that of H. A value of $2.97 \cdot 10^{-12} \text{ cm}^3 \text{ molecule}^{-1} \text{ s}^{-1}$ was obtained, which agrees well with the experimen-

System	$k(T)$ [$\text{cm}^3 \text{ molecule}^{-1} \text{ s}^{-1}$]		
	This work	Experimental	Other theoretical
H + ClF \rightarrow HF + Cl	$11.6 \cdot 10^{-12}$	$7.4 \cdot 10^{-12}$ [27] (12.0 ± 1.0) $\cdot 10^{-12}$ [26] $5.2 \cdot 10^{-12}$ [28]	$(6.7 \pm 0.10) \cdot 10^{-12}$ [11]
D + ClF \rightarrow DF + Cl	$2.97 \cdot 10^{-12}$	$(3.3 \pm 0.4) \cdot 10^{-12}$ [26]	$(5.16 \pm 0.22) \cdot 10^{-12}$ [11]
H + ClF \rightarrow HCl + F	$3.03 \cdot 10^{-11}$	$3.2 \cdot 10^{-11}$ [27] (2.9 ± 0.3) $\cdot 10^{-11}$ [26] $3.5 \cdot 10^{-11}$ [28]	$(2.65 \pm 0.04) \cdot 10^{-11}$ [11]
D + ClF \rightarrow DCl + F	$2.34 \cdot 10^{-11}$	$(2.8 \pm 0.2) \cdot 10^{-11}$ [26]	$(2.01 \pm 0.04) \cdot 10^{-11}$ [11]
H + ICl \rightarrow HCl + I	$4.76 \cdot 10^{-11}$	$4.94 \cdot 10^{-11}$ [29]	
H + F ₂ \rightarrow HF + F	$3.59 \cdot 10^{-12}$	$1.1 \cdot 10^{-12}$ [29] $3.65 \cdot 10^{-12}$ [30] $2.98 \cdot 10^{-12}$ [31] $1.59 \cdot 10^{-12}$ [32]	
H + Cl ₂ \rightarrow HCl + Cl	$2.46 \cdot 10^{-11}$	$2.06 \cdot 10^{-11}$ [29]	
F + HCl \rightarrow HF + Cl	$8.82 \cdot 10^{-12}$	$(8.1 \pm 0.5) \cdot 10^{-12}$ [33] (8.2 ± 0.9) $\cdot 10^{-12}$ [34] (7.2 ± 0.5) $\cdot 10^{-12}$ [35]	$(7.87 \pm 0.12) \cdot 10^{-12}$ [11]
F + DCl \rightarrow DF + Cl	$7.83 \cdot 10^{-12}$	$(6.0 \pm 0.7) \cdot 10^{-12}$ [34]	$(4.35 \pm 0.16) \cdot 10^{-12}$ [11]
F + HBr \rightarrow HF + Br	$4.38 \cdot 10^{-11}$	$(4.5 \pm 0.4) \cdot 10^{-11}$ [36]	
F + HI \rightarrow HF + I	$4.08 \cdot 10^{-11}$	$(4.09 \pm 0.08) \cdot 10^{-11}$ [36]	
F + H ₂ \rightarrow HF + H	$7.06 \cdot 10^{-12}$		$(6.2 \pm 0.4) \cdot 10^{-12}$ [16]
Cl + HD \rightarrow HCl + D	$2.42 \cdot 10^{-14}$		$2.23 \cdot 10^{-14}$ [6]
Cl + DH \rightarrow DCl + H	$7.82 \cdot 10^{-14}$		$8.95 \cdot 10^{-15}$ [6]
Cl + H ₂ \rightarrow HCl + H	$1.83 \cdot 10^{-14}$		$(1.8 \pm 0.3) \cdot 10^{-14}$ [16] $2.29 \cdot 10^{-14}$ [37]

Table 2. Calculated and experimental rate constants. Numbers in brackets are reference numbers. Rate constants obtained in this work have an estimated error of 3%.

tal rate of $(3.3 \pm 0.4) \cdot 10^{-12} \text{ cm}^3 \text{ molecule}^{-1} \text{ s}^{-1}$, obtained by Bykhalo and coworkers [26]. Our results agree better with the experiment than the one obtained theoretically by Sayos et al. [11]. Comparing our rates of H and D with ClF yields a ratio of 3.9, which is within the range of the experimental ratio (3.0–4.5) [26]. This agreement increases the faith in the accuracy of the method applied in the present work.

C) H + ClF \rightarrow HCl + F

The colliding particles here are the same as in reaction H + ClF \rightarrow HF + Cl, but with the formation of HCl instead of HF. The purpose of studying this system is to compare probabilities of formation of the two molecules HCl vs. HF. The calculations were performed under the same initial conditions as in reaction 3.1.A. The probability of the formation of HCl is 0.0954, and its rate constant is $3.03 \cdot 10^{-11} \text{ cm}^3 \text{ molecule}^{-1} \text{ s}^{-1}$. These are almost *three* times larger than the corresponding values for the formation of HF. Looking at (22), with D_{HCl} is generally smaller than D_{HF} , gives a potential value V_{HCl} larger than V_{HF} at any distance throughout the trajectory, which means a stronger attraction and hence a favourable formation of HCl over HF. The experimental [26] ratio of the rate constants for the formation of

HCl vs. HF is the same as the calculated ratio. The same agreement is also observed in the experimental findings reported by Setser et al. [29]. From the relative infrared emission intensities of HCl and HF produced by the H + ClF reaction, they found a macroscopic branching ratio of 5.2 favouring the HCl channel. Comparing our calculated rate constant with other calculated values [11] shows a reasonable agreement, as shown in Table 2.

D) D + ClF \rightarrow DCl + F

The calculated rate constant, at the same initial conditions as in previous reactions, is $2.34 \cdot 10^{-11} \text{ cm}^3 \text{ molecule}^{-1} \text{ s}^{-1}$. This agrees well with the experimental value [26] and with other theoretical calculations [11]. For the reactions H + ClF \rightarrow HCl + F and D + ClF \rightarrow DCl + F, the calculated rate constant predicts a small isotope effect, i. e. $k_{(\text{H}+\text{ClF})}/k_{(\text{D}+\text{ClF})} = 1.29$, which agrees well with the range of experimental values [26] of 0.87–1.23 and with other theoretical calculations [11] of 1.32.

E) H + ICl \rightarrow HCl + I

Due to the large size of the iodine atom, the calculated reaction cross-section, hence the rate constant, for this reaction is expected to be larger than the rate

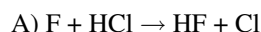
constant for the corresponding reaction $\text{H} + \text{ClF} \rightarrow \text{HCl} + \text{F}$. A value of $4.76 \cdot 10^{-11} \text{ cm}^3 \text{ molecule}^{-1} \text{ s}^{-1}$ was obtained. This agrees well with the experimental results of $4.94 \cdot 10^{-11} \text{ cm}^3 \text{ molecule}^{-1} \text{ s}^{-1}$ reported by Setser et al. [29].



To study the effect of a diatomic molecule on the reaction rate, the reaction of a hydrogen atom with both F_2 and Cl_2 were studied. The calculated rate constants for the formation of HF and HCl were found to be $3.59 \cdot 10^{-12}$ and $2.46 \cdot 10^{-11} \text{ cm}^3 \text{ molecule}^{-1} \text{ s}^{-1}$, respectively. The Cl-Cl bond is a weaker bond than the F-F bond. Therefore, one would expect a higher rate constant for HCl formation compared with HF formation. This is in accord with our findings. Comparing the calculated rate constants with those obtained experimentally [29–32], good agreements are observed, as shown in Table 2. Comparing the ratio of $k_{(\text{H}+\text{F}_2)}/k_{(\text{H}+\text{Cl}_2)} = 0.146$ found in the present work with the range of experimental data (0.053–0.177) shows a satisfying agreement between calculations and experiments.

3.2. Reactions of Fluorine Atoms with Different Diatomic Molecules

To study the effect of the nature of the isolated atom A on the reactive collision with the BC molecule, the rate constant for the reaction of F atoms with various diatomic molecules have been studied. Simple hydrogen halide molecules (HX, where X = Cl, Br, I) were selected for the study. Effects of various parameters on rates are discussed below.

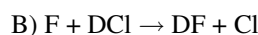


The calculated reaction probability and cross-section for this reaction are listed in Table 1. At 300 K, the calculated rate constant was found to be $8.82 \cdot 10^{-12} \text{ cm}^3 \text{ molecule}^{-1} \text{ s}^{-1}$. Several investigators studied this reaction experimentally. Wurzberg et al. [33, 34] reported rate constants of $(8.1 \pm 0.5) \cdot 10^{-12}$ and $(8.2 \pm 0.9) \cdot 10^{-12} \text{ cm}^3 \text{ molecule}^{-1} \text{ s}^{-1}$. Moore et al. [35] reported a value of $(7.2 \pm 0.5) \cdot 10^{-12} \text{ cm}^3 \text{ molecule}^{-1} \text{ s}^{-1}$. The agreement between our calculated value and the experimental ones is obvious. This reaction was also studied theoretically by Sayos et al. [11]. With the same set of initial conditions as in the present work, they reported a rate constant of $(7.87 \pm 0.12) \cdot 10^{-12} \text{ cm}^3 \text{ molecule}^{-1} \text{ s}^{-1}$. The agreement with our rate constant is obvious.

Table 3. Calculated and experimental rate constants for the reaction $\text{F} + \text{HCl} \rightarrow \text{HF} + \text{Cl}$ at different temperatures. Numbers in brackets are reference numbers. Rate constants obtained in this work have an estimated error of 3%.

T [K]	$k(T)$ [$\text{cm}^3 \text{ molecule}^{-1} \text{ s}^{-1}$]	
	This work	Experimental
194	$5.94 \cdot 10^{-12}$	$(6.92 \pm 0.68) \cdot 10^{-12}$ [33]
223	$6.85 \cdot 10^{-12}$	$(7.27 \pm 0.43) \cdot 10^{-12}$ [33]
270	$7.86 \cdot 10^{-12}$	$(7.52 \pm 0.70) \cdot 10^{-12}$ [33]
298	$8.57 \cdot 10^{-12}$	$(8.07 \pm 0.5) \cdot 10^{-12}$ [36]

The dependence of the rate constant on the temperature was studied. The calculated and the experimental rate constants at various temperatures are shown in Table 3. The agreement between the two rates over a temperature range is clear.



The calculated rate constant for this reaction at 300 K equals $7.83 \cdot 10^{-12} \text{ cm}^3 \text{ molecule}^{-1} \text{ s}^{-1}$, which agrees reasonably with both experimental [34] and other theoretical work [11], as shown in Table 2. For the reactions $\text{F} + \text{HCl} \rightarrow \text{HF} + \text{Cl}$ and $\text{F} + \text{DCl} \rightarrow \text{DF} + \text{Cl}$, the calculated rate constants predict a small isotope effect, i. e. $k_{(\text{H})}/k_{(\text{D})} = 1.13$, which matches well with both the experimental ratio [34], $k_{(\text{H})}/k_{(\text{D})} = 1.37$, and the theoretical ratio, $k_{(\text{H})}/k_{(\text{D})} = 1.81$, found by other investigators [11].



The reaction probabilities and cross-sections for these two reactions are shown in Table 1. The calculated rate constants were found to be $4.38 \cdot 10^{-11} \text{ cm}^3 \text{ molecule}^{-1} \text{ s}^{-1}$ (at 297 K) for the $\text{F} + \text{HBr}$ reaction and $4.08 \cdot 10^{-11} \text{ cm}^3 \text{ molecule}^{-1} \text{ s}^{-1}$ (at 293 K) for the $\text{F} + \text{HI}$ reaction. The two rate constants have comparable values due to the comparability of their spectroscopic constants. This agrees with what was observed experimentally [36], as shown in Table 2.

3.3. Reactions of Fluorine and Chlorine Atoms with Hydrogen Molecules



Reaction probabilities, cross-sections and rate constants for these two reactions were calculated at various temperatures. At 300 K, the reaction probabilities and cross-sections are shown in Table 1. According to our discussion above (reaction $\text{H} + \text{ClF} \rightarrow \text{HCl} + \text{F}$), regarding the Morse potential well depths for HF and

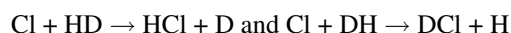
T [K]	$k(T)$ [cm ³ molecule ⁻¹ s ⁻¹]				
	F + H ₂ → HF + H		Cl + H ₂ → HCl + H		
	This work	Others [16]	This work	Others [16]	Others [37]
200	6.30 · 10 ⁻¹²	(2.0 ± 0.1) · 10 ⁻¹²	1.34 · 10 ⁻¹⁵	—	—
250	6.71 · 10 ⁻¹²	(4.0 ± 0.3) · 10 ⁻¹²	5.27 · 10 ⁻¹⁵	(5.3 ± 1.5) · 10 ⁻¹⁵	5.74 · 10 ⁻¹⁵
300	7.06 · 10 ⁻¹²	(6.2 ± 0.4) · 10 ⁻¹²	1.83 · 10 ⁻¹⁴	(1.8 ± 0.3) · 10 ⁻¹⁴	2.29 · 10 ⁻¹⁴
400	—	—	0.994 · 10 ⁻¹³	(1.1 ± 0.1) · 10 ⁻¹³	1.27 · 10 ⁻¹³
500	12.5 · 10 ⁻¹²	(14.0 ± 0.0) · 10 ⁻¹²	2.78 · 10 ⁻¹³	(3.7 ± 0.4) · 10 ⁻¹³	3.99 · 10 ⁻¹³
600	—	—	6.91 · 10 ⁻¹³	(7.4 ± 0.8) · 10 ⁻¹³	8.53 · 10 ⁻¹³
1000	34.8 · 10 ⁻¹²	(34.0 ± 0.1) · 10 ⁻¹²	5.54 · 10 ⁻¹²	(4.8 ± 0.4) · 10 ⁻¹²	—

Table 4. Calculated rate constants for the reactions F + H₂ → HF + H and Cl + H₂ → HCl + H at different temperatures. Rate constants obtained in this work have an estimated error of 3%.

HCl molecules, one would expect a higher probability of formation for HCl than HF. This is what was found in the calculations as shown in Table 1. The rate constants of HF and HCl formation were calculated over a wide temperature range (200–1000 K). Results of our calculations along with calculated rates, obtained by other investigators [16, 37], are shown in Table 4. Even though both the reaction probability and cross-section of HCl formation are higher than that for HF, the rate constant for the reaction Cl + H₂ → HCl + H is between 1–3 orders of magnitude smaller than that for the F + H₂ → HF + H reaction. The reaction of H₂ with Cl is a largely endothermic process, contrary to its reaction with the F atom. This makes the reaction with Cl much affected by the temperature. Its rate constant increases by more than 4000 times between 200 K and 1000 K, while the increment in the reaction rate with F is only about five-fold over the same temperature range. To compensate for the endothermicity of the Cl + H₂ reaction, a literature value [6] of the barrier energy, $E_0 = 0.172$ eV, was included in the calculations of the rate constant using (40). The agreement between our calculated rate constants and those reported by other researchers is obvious over a wide range of temperatures.

3.4. Reactions of Chlorine Atoms with Hydrogen Molecules and their Isotope Analogues

The reaction of chlorine atoms with hydrogen molecules is an endothermic process. A barrier energy has to be included in the calculations of the rate constant, as indicated in (40). Effects of temperature and barrier energy on reactions rates were studied.



The barrier energies for these two endothermic reactions are [6]: 0.156 eV and 0.210 eV, respectively. The reaction probabilities and cross-sections are shown in Table 1. At 300 K, their calculated rate constants,

Table 5. Calculated rate constants for the reactions Cl + HD → HCl + D and Cl + DH → DCl + H at different temperatures. Rate constants obtained in this work have an estimated error of 3%.

T [K]	$k(T)$ [cm ³ molecule ⁻¹ s ⁻¹]			
	Cl + HD → HCl + D		Cl + DH → DCl + H	
	This work	Others [6]	This work	Others [6]
250	6.61 · 10 ⁻¹⁵	5.73 · 10 ⁻¹⁵	1.48 · 10 ⁻¹⁵	1.76 · 10 ⁻¹⁵
300	2.42 · 10 ⁻¹⁴	2.23 · 10 ⁻¹⁴	7.82 · 10 ⁻¹⁵	8.95 · 10 ⁻¹⁵
400	1.24 · 10 ⁻¹³	1.29 · 10 ⁻¹³	6.62 · 10 ⁻¹⁴	7.27 · 10 ⁻¹⁴
500	3.46 · 10 ⁻¹³	3.87 · 10 ⁻¹³	2.22 · 10 ⁻¹³	2.67 · 10 ⁻¹³

in units of cm³ molecule⁻¹ s⁻¹, are: 2.42 · 10⁻¹⁴ and 7.82 · 10⁻¹⁴. The higher barrier energy for the formation of DCl, compared with that for HCl, explains its smaller rate. The rate constant for these two reactions were calculated at several temperatures. Due to its higher endothermicity, the rate constant for DCl formation increases by 150 times by doubling the temperature from 250 K to 500 K. Over the same temperature range, the rate constant for HCl formation increases only 50-fold. Results are shown in Table 5 along with rates calculated by other researchers [6] for comparison. Good agreement is observed over a wide temperature range.

A comparison can also be made with results obtained for the reaction: Cl + H₂ → HCl + H, discussed before. The spectroscopic constants and Morse potential parameters of this reaction predict intermediate values for reaction probability and cross-section, compared to the previous two reactions, as shown in Table 1. Also, with a barrier energy of 0.172 eV, one would expect to have an intermediate value for the rate constant. At 300 K, its rate constant of 1.83 · 10⁻¹⁴ cm³ molecule⁻¹ s⁻¹ is larger than the rate constant of Cl + DH → DCl + H, but smaller than that for the Cl + HD → HCl + D reaction.

4. Conclusions

Reaction probabilities, cross-sections and rate constants for atom-diatomic molecule collisions have

been studied in three dimensions using Monte Carlo classical trajectories. Morse potential energy surfaces were applied to describe interactions between colliding particles. Various atoms and various diatomic molecules were used in the study. For some systems, calculations were performed at several temperatures. A strong dependence has been found on the nature of the interacting particles (with different spectroscopic constants and potential parameters), temperature of the reaction and the nature of the reaction (endothermicity and exothermicity). The results of calculations were compared with experimental val-

ues and with values obtained by other researchers using different calculation methods. On the overall, an excellent agreement was observed with experimental results. A reasonable and acceptable agreement was also observed with works of other investigators who applied different calculation methods. These findings should improve our understanding of the dynamical mechanism of reactions in the collision process. Also, classical trajectory calculations shall provide a trustful alternative method to the tedious and costly way of evaluating rate constants experimentally.

- [1] C. Zuhrt, F. Schneider, U. Havemann, L. Ziilicke, and Z. Herman, *Chem. Phys.* **38**, 205 (1979).
- [2] W. A. Lester Jr. and R. Schinke, *J. Chem. Phys.* **70**, 4893 (1979).
- [3] A. C. Luntz, R. Schinke, W. A. Lester Jr., and H. H. Günthard, *J. Chem. Phys.* **70**, 5908 (1979).
- [4] E. Herbst, L. G. Payne, R. L. Champion, and L. D. Doverspike, *Chem. Phys.* **42**, 413 (1979).
- [5] R. L. Jaffe, *Chem. Phys.* **40**, 185 (1979).
- [6] A. Persky, *J. Chem. Phys.* **70**, 3910 (1979).
- [7] T. Yamamoto and W. H. Miller, *J. Chem. Phys.* **118**, 2135 (2003).
- [8] R. S. Judson, S. Shi, and H. Rabitz, *J. Chem. Phys.* **90**, 2263 (1989).
- [9] D. L. Thompson, R. E. Howard, and L. Mansker, *Chem. Phys. Lett.* **127**, 398 (1986).
- [10] J. S. Hutchinson and R. E. Wyatt, *J. Chem. Phys.* **70**, 3509 (1979).
- [11] R. Sayos, J. Hernando, R. Francia, and M. Gonzalez, *Phys. Chem. Chem. Phys.* **2**, 523 (2000).
- [12] D. G. Truhlar, *J. Phys. Chem.* **83**, 188 (1979).
- [13] F. L. Paul, S. Y. Grebenshchikov, and R. Schinke, *J. Chem. Phys.* **119**, 4700 (2003).
- [14] J. C. Gray and D. G. Truhlar, *J. Phys. Chem.* **83**, 1045 (1979).
- [15] J. N. L. Connor, W. Jakubetz, and A. Lagana, *J. Phys. Chem.* **83**, 73 (1979).
- [16] J. T. Muckerman and M. B. Faist, *J. Phys. Chem.* **83**, 79 (1979).
- [17] R. N. Porter, M. Karplus, and R. D. Sharma, *J. Chem. Phys.* **43**, 3259 (1965).
- [18] F. J. Aoiz, V. J. Herrero, and V. S. Rabanos, *J. Chem. Phys.* **94**, 7991 (1991).
- [19] H. M. Abdel-Halim and B. I. Al-Shihi, *Indian J. Chem.* **35**, 366 (1996).
- [20] D. L. Bunker, *Methods Comput. Phys.* **10**, 287 (1971).
- [21] P. W. Atkins, *Physical Chemistry*, Oxford University Press, Oxford 1994, chapter 27.
- [22] J. I. Steinfeld, J. S. Francisco, and W. L. Hase, *Chemical Kinetics and Dynamics*, Prentice Hall, Upper Saddle River, NJ 1998, chapter 8.
- [23] Revised Nuffield Advanced Science, *Book of Data*, Longman, Harlow 1984, pp.18–22.
- [24] K. P. Huber and G. Herzberg, *Molecular Spectra and Molecular Structures*, Von Nostrand, New York 1979.
- [25] <http://physics.nist.gov/cgi-bin/MolSpec/mole>
- [26] I. B. Bykhalo, V. V. Filatov, E. B. Gordon, and A. P. Perminov, *Russ. Chem. Bull.* **43**, 1637 (1994).
- [27] K. Tamagake and D. W. Setser, *J. Phys. Chem.* **83**, 1000 (1979).
- [28] D. Brandt and J. C. Polanyi, *Chem. Phys.* **35**, 23 (1978).
- [29] D. W. Setser, J. P. Sung, and R. J. Malins, *J. Phys. Chem.* **83**, 1007 (1979).
- [30] R. G. Albright, A. F. Dodonov, G. K. Lavrovskaya, I. I. Morosov, and V. L. Talroz, *J. Chem. Phys.* **50**, 3632 (1969).
- [31] J. B. Levy and B. S. W. Copeland, *J. Phys. Chem.* **72**, 3168 (1968).
- [32] K. H. Homann, H. Schweinfurt, and J. Warnatz, *Ber. Bunsenges. Phys. Chem.* **81**, 724 (1977).
- [33] E. Wurzberg and P. L. Houston, *J. Chem. Phys.* **72**, 5915 (1980).
- [34] E. Wurzberg, A. J. Grimley, and P. L. Houston, *Chem. Phys. Lett.* **57**, 373 (1978).
- [35] C. M. Moore, I. W. M. Smith, and D. W. A. Stewart, *Int. J. Chem. Kinet.* **26**, 813 (1994).
- [36] J. C. Weisshaar, T. S. Zwier, and S. R. Leone, *J. Chem. Phys.* **75**, 4873 (1981).
- [37] A. Persky, *J. Chem. Phys.* **66**, 2932 (1977).